Journal of Statistical Physics (2020) 178:625–643
https://doi.org/10.1007/s10955-019-02446-6

Span Observables: "When is a Foraging Rabbit No Longer Hungry?"

Kay Jörg Wiese[1]

Received: 8 September 2019 / Accepted: 16 November 2019 / Published online: 30 November 2019

Abstract
Be X_t a random walk. We study its span S, i.e. the size of the domain visited up to time t. We want to know the probability that S reaches 1 for the first time, as well as the density of the span given t. Analytical results are presented, and checked against numerical simulations. We then generalize this to include drift, and one or two reflecting boundaries. We also derive the joint probability of the maximum and minimum of a process. Our results are based on the diffusion propagator with reflecting or absorbing boundaries, for which a set of useful formulas is derived.

Keywords Span · Random walk · Diffusion · First passage

1 Introduction

Consider a Brownian motion X_t, starting at $X_0 = 0$, with drift μ, and variance 2,

$$\langle X_t \rangle = \mu t \ . \tag{1}$$

$$\left\langle \left(X_t - \langle X_t \rangle \right)^2 \right\rangle = 2t \ . \tag{2}$$

A sample trajectory is sketched on Fig. 1 (for $\mu = 0$). A key problem in stochastic processes are the first-passage properties [1–3] in a finite domain, say the unit interval [0, 1]. For a Brownian, the probability to exit at the upper boundary $x = 1$ without visiting the lower boundary at $x = 0$, while starting at x is

$$P_1(x) = x \ . \tag{3}$$

Another key observable is the exit time, starting at x, which behaves as $\langle T_{\rm exit}(x) \rangle_0 \sim x(1-x)$.

Communicated by Giulio Biroli.

Kay Jörg Wiese
wiese@lpt.ens.fr

1 Laboratoire de Physique de l'Ecole Normale Supérieure, ENS, Université PSL, CNRS, Sorbonne Université, Université Paris-Diderot, Sorbonne Paris Cité, Paris, France

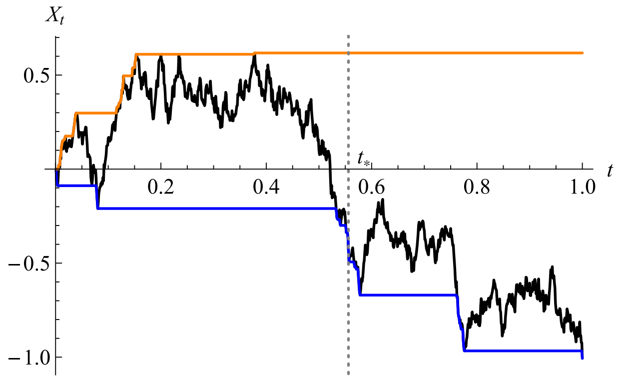

Fig. 1 The random process X_t, with its running max (in orange) and min (in blue) (Color figure online)

Here we consider a different set of observables, namely the *span* of a process: define the positive and negative records (a.k.a. the running max and min) as

$$M_+(t) := \max_{t' \leq t} X_{t'} \ , \tag{4}$$

$$M_-(t) := \min_{t' \leq t} X_{t'} \ . \tag{5}$$

These observables are drawn on Fig. 1. The span $S(t)$ is their difference, i.e. the size of the (compact) domain visited up to time t (Fig. 2),

$$S(t) := M_+(t) - M_-(t) \ . \tag{6}$$

We study the probability that $S(t)$ becomes 1 for the first time. Curiously, this observable is rarely treated in the literature, and most of the studies we found are concerned with questions of convergence of the first moments, which is non-trivial when the process is more complicated than a Brownian motion: Let us mention the mean first-passage time [4], with some discrepancies stated in Ref. [5]. The full distribution as a function of times is derived below. A related but distinct observable is the density of the span at time t, considered in the classic references [5–8]. A beautiful recent result is the covariance of the span [9].

One may ask where span observables actually occur in nature? One example is the *Hungry Rabbit Problem*. Suppose a hungry and myopic rabbit is released. It will perform a Brownian motion, until its stomach is full, i.e. the span of its trajectory reaches 1. This is a variant of the myopic rabbit introduced in [10]. We will give the probability for the time that the rabbit is no longer hungry analytically, including some drift in the rabbit's motion, when e.g. it prefers to move downhill. In a further twist, there can be reflecting walls restricting the rabbits movement, corresponding to Neumann boundary conditions for the Brownian motion. One may object that the problem is not realistic, since foraging the rabbit consumes food. We currently have no solution for the latter problem, even though diffusion with moving boundaries can, at least in principle, be treated via a set of integral equations [11]; however we do not know of a closed-form solution. A notable exception are expanding boundaries in the limit of large times, where the survival probability can be evaluated analytically [12].

Another example arises in measuring the exit probability from the strip [0, 1], starting at x. This problem was studied for fractional Brownian motion in Ref. [13]. The question is how long one has to run a simulation until the process $X_t + x$ has exited from the unit interval

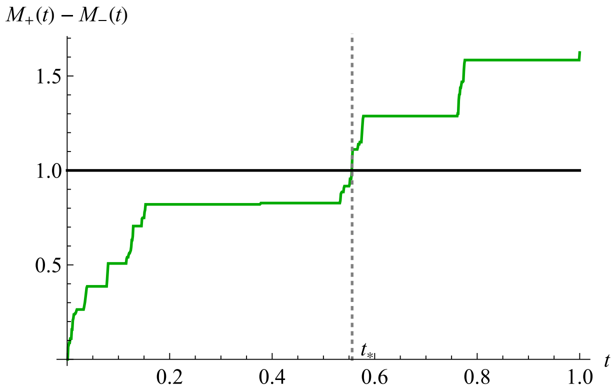

Fig. 2 The span $S(t) := M_+(t) - M_-(t)$ of X_t from Fig. 1

[0, 1], for all $x \in [0, 1]$. We claim that the simulation can be stopped at time t_* when the span first reaches 1. To understand this statement, define x_* as minus the running minimum $M_-(t)$ given in Eq. (5)

$$x_* := -M_-(t_*) \ . \tag{7}$$

Then for $t \leq t_*$ one has

$$\min_{0 \leq t \leq t_*} X_t + x_* = 0 \text{ and } \max_{0 \leq t \leq t_*} X_t + x_* = 1 \tag{8}$$

$$\Longrightarrow \min_{0 \leq t \leq t_*} X_t + x > 0 \text{ and } \max_{0 \leq t \leq t_*} X_t + x > 1 \text{ for } x > x_* \tag{9}$$

$$\Longrightarrow \min_{0 \leq t \leq t_*} X_t + x < 0 \text{ and } \max_{0 \leq t \leq t_*} X_t + x < 1 \text{ for } x < x_* \tag{10}$$

The interpretation is as follows: a process starting at $x > x_*$ first reaches the upper boundary $x = 1$ before reaching the lower boundary at $x = 0$, while a process starting at $x < x_*$ first reaches the lower boundary. Finally, for $t < t_*$ there exist x for which one cannot decide.

A related quantity is the joint density of the running maximum and minimum, given t. This question is relevant in the analysis of stock-market data [14], where it allows one to quantify violations of the Markov property.

The span is also relevant in the search of a protein for its binding site on a DNA molecule. The idea of *facilitated diffusion* [15] is to alternatively diffuse along the DNA molecule or in 3d space, thus optimizing the search.

We also consider reflecting boundary conditions for the Brownian motion. These have different physical interpretations: For the myopic rabbit introduced above, they are hard walls it cannot penetrate. For diffusion on a 1-dimensional object, as an DNA molecule, these are the ends of the molecule. In financial markets, these may be bounds at which an investor takes out, or has to reintroduce cash.

Finally, the span is not a Markov process, but a process with memory, as it remembers its positive and negative records. This places our study in the larger context of processes with memory, of which fractional Brownian motion may be the most relevant one [16–19].

The remainder of this article is organized as follows: we first derive key results for Brownian motion in the unit interval [0, 1], with absorbing boundary conditions at both ends, see Sect. 2. This is then generalized to one absorbing and one reflecting boundary in Sect. 3, and to two reflecting ones in Sect. 4. Most of these results are known. We give analytical results for span observables in Sect. 5, and the joint distribution of running maximum and minimum in Sect. 6. A generalization to a Brownian motion with one reflecting boundary is presented in Sect. 7, while two reflecting boundaries are treated in Sect. 8. We conclude in Sect. 9 with open problems.

2 Basic Formulas for Brownian Motion with Two Absorbing Boundaries

2.1 Solving the Fokker–Planck Equation

Consider a Brownian motion $X(t)$ given by its Langevin equation

$$\partial_t X_t = \mu + \eta_t \ , \qquad \langle \eta_t \eta_{t'} \rangle = 2\delta(t-t') \ . \tag{11}$$

There are absorbing (Dirichlet) boundary conditions both at $x = 0$, and $x = 1$. If the trajectory starts at $X_0 = x$, and ends at $X_t = y$, then the forward Fokker–Planck equation reads [1–3]

$$\partial_t P^{\mu}_{\rm DD}(x,y,t) = \frac{\partial^2}{\partial y^2} P^{\mu}_{\rm DD}(x,y,t) - \mu \frac{\partial}{\partial y} P^{\mu}_{\rm DD}(x,y,t) \ . \tag{12}$$

The index "DD" refers to the two absorbing (Dirichlet) boundary conditions at $x = 0$, and $x = 1$. The probability to survive at time t is given by $\int_0^1 \mathrm{d}y\, P_{\rm DD}(x,y,t)$. The general solution of the Fokker–Planck equation (12) can be written as

$$P^{\mu}_{\rm DD}(x,y,t) = \mathrm{e}^{\frac{\mu(y-x)}{2} - \frac{\mu^2 t}{4}} \left[\mathbb{P}(x-y,t) - \mathbb{P}(x+y,t)\right] \ . \tag{13}$$

The key object in this construction is

$$\mathbb{P}(z,t) := \frac{1}{\sqrt{4\pi t}} \sum_{n=-\infty}^{\infty} \mathrm{e}^{-(z+2n)^2/4t} = \frac{1}{2}\vartheta_3\Big(\frac{\pi}{2}z, \mathrm{e}^{-\pi^2 t}\Big) . \tag{14}$$

ϑ is the elliptic ϑ-function. Using the Poisson summation formula, an alternative form for $\mathbb{P}(z,t)$ is

$$\mathbb{P}(z,t) = \frac{1}{2} + \sum_{m=1}^{\infty} \mathrm{e}^{-m^2\pi^2 t} \cos(m\pi z) \ . \tag{15}$$

To prove the above statements it is enough to remark that Eq. (13) satisfies the Fokker–Planck equation (12), vanishes at $y = 0$ and $y = 1$, and reduces for $t \to 0$ to a δ-function

$$\lim_{t\to 0} P^{\mu}_{+}(x,y,t) = \delta(x-y) \ . \tag{16}$$

The function $\mathbb{P}(z,t)$ has the following properties

$$\mathbb{P}(z,t) = \mathbb{P}(z+2,t) = \mathbb{P}(-z,t) \ . \tag{17}$$

As a consequence,

$$\partial_z \mathbb{P}(z,t)\big|_{z=\rm integer} = 0 \tag{18}$$

It is useful to consider its Laplace-transformed version. We define the Laplace transform of a function $F(t)$, with $t \geq 0$, and marked with a tilde as

$$\tilde{F}(s) := \mathcal{L}_{t\to s}\left[F(t)\right] = \int_0^{\infty} \mathrm{d}t\, \mathrm{e}^{-st} F(t) \ . \tag{19}$$

(Note that we use s for the Laplace variable, and S for the span.) This yields for $-2 < z < 2$

$$\begin{aligned}\tilde{\mathbb{P}}(z, s) &= \frac{\mathrm{e}^{-\sqrt{s}|z|}}{2\sqrt{s}} + \frac{\left[\coth(\sqrt{s}) - 1\right]\cosh(\sqrt{s}z)}{2\sqrt{s}} \\ &= \frac{1}{2s} + \frac{1}{12}(2 - 6|z| + 3z^2) + \frac{s}{720}\left(-60z^2|z| + 15\left(z^2+4\right)z^2 - 8\right) + \dots\end{aligned} \tag{20}$$

And

$$\mathcal{L}_{t\to s}\left[\mathrm{e}^{-\frac{\mu^2 t}{4}}\mathbb{P}(z, t)\right] = \tilde{\mathbb{P}}\left(z, s + \frac{\mu^2}{4}\right). \tag{21}$$

Note that the combination in square brackets in Eq. (13) can be written as

$$\begin{aligned}\mathbb{P}(x - y, t) - \mathbb{P}(x + y, t) = &\frac{\mathrm{e}^{-\sqrt{s}|x-y|} - \mathrm{e}^{-\sqrt{s}(x+y)}}{2\sqrt{s}} \\ &- \frac{\left[\coth(\sqrt{s}) - 1\right]\sinh(\sqrt{s}x)\sinh(\sqrt{s}y)}{\sqrt{s}}.\end{aligned} \tag{22}$$

The form (22) facilitates its integration over x and y, which is useful when concatenating several propagators [13].

2.2 Boundary Currents and Conservation of Probability

Conservation of probability reads (the variable x is the initial condition, here a dummy variable)

$$\partial_t P^{\mu}_{\mathrm{DD}}(x, y, t) + \partial_y J^{\mu}_{\mathrm{DD}}(x, y, t) = 0\,. \tag{23}$$

J^{μ}_{DD} is the current, which from Eqs. (12), (13) and (23) can be identified as

$$\begin{aligned}J^{\mu}_{\mathrm{DD}}(x, y, t) &= (\mu - \partial_y)P^{\mu}_{\mathrm{DD}}(x, y, t) \\ &= \mathrm{e}^{\frac{\mu(y-x)}{2} - \frac{\mu^2 t}{4}}\left(\frac{\mu}{2} - \partial_y\right)\left[\mathbb{P}(x - y, t) - \mathbb{P}(x + y, t)\right]\,.\end{aligned} \tag{24}$$

Due to the Dirichlet conditions at $y = 0$ and $y = 1$, we have

$$\int_0^1 \mathrm{d}y\, \partial_t P^{\mu}_{\mathrm{DD}}(x, y, t) = J^{\mu}_{\mathrm{DD}}(x, 0, t) - J^{\mu}_{\mathrm{DD}}(x, 1, t)\,. \tag{25}$$

Thus, the probability to exit at time t, when starting in x at time 0 reads

$$\begin{aligned}P^{\mathrm{DD}}_{\mathrm{exit}}(x, t) &= J^{\mu}_{\mathrm{DD}}(x, 1, t) - J^{\mu}_{\mathrm{DD}}(x, 0, t) \\ &= 2\,\mathrm{e}^{-\frac{\mu^2 t}{4}}\left[\mathrm{e}^{\frac{\mu(1-x)}{2}}\partial_x\mathbb{P}(1 - x, t) - \mathrm{e}^{-\frac{\mu x}{2}}\partial_x\mathbb{P}(x, t)\right].\end{aligned} \tag{26}$$

The outgoing currents at the upper and lower boundary are

$$J^{\mu}_{\mathrm{DD}}(x, 1, t) = 2\,\mathrm{e}^{-\frac{\mu^2 t}{4}}\,\mathrm{e}^{\frac{\mu(1-x)}{2}}\,\partial_x\mathbb{P}(1 - x, t)\,, \tag{27}$$

$$-J^{\mu}_{\mathrm{DD}}(x, 0, t) = -2\,\mathrm{e}^{-\frac{\mu^2 t}{4}}\,\mathrm{e}^{-\frac{\mu x}{2}}\,\partial_x\mathbb{P}(x, t)\,. \tag{28}$$

The Laplace transforms of these outgoing currents are

$$-\tilde{J}^{\mu}_{\rm DD}(x,0,s) = \mathrm{e}^{-\frac{\mu x}{2}} \left.\frac{\sinh\left(\sqrt{s'}(1-x)\right)}{\sinh(\sqrt{s'})}\right|_{s'=s+\mu^2/4}, \tag{29}$$

$$\tilde{J}^{\mu}_{\rm DD}(x,1,s) = \mathrm{e}^{\frac{\mu(1-x)}{2}} \left.\frac{\sinh(\sqrt{s'}\,x)}{\sinh(\sqrt{s'})}\right|_{s'=s+\mu^2/4}. \tag{30}$$

2.3 Absorption Probabilities at $x = 0$ and $x = 1$

The absorption probabilities at $x = 0$ and $x = 1$ are

$$\begin{aligned} P^{\mu}_{\rm DD,0}(x) &:= \int_0^\infty \mathrm{d}t\, \left[-J^{\mu}_{\rm DD}(x,0,t)\right] = \lim_{s\to 0}\left[-\tilde{J}^{\mu}_{\rm DD}(x,0,s)\right] \\ &= \mathrm{e}^{-\frac{\mu x}{2}} \frac{\sinh\left(\frac{\mu}{2}(1-x)\right)}{\sinh\left(\frac{\mu}{2}\right)}, \end{aligned} \tag{31}$$

$$\begin{aligned} P^{\mu}_{\rm DD,1}(x) &:= \int_0^\infty \mathrm{d}t\, J^{\mu}_{\rm DD}(x,1,t) = \lim_{s\to 0} \tilde{J}^{\mu}_{\rm DD}(x,1,s) \\ &= \mathrm{e}^{-\frac{1}{2}\mu(x-1)} \frac{\sinh\left(\frac{\mu x}{2}\right)}{\sinh\left(\frac{\mu}{2}\right)}. \end{aligned} \tag{32}$$

2.4 Moments of the Absorption Time, Starting at x

Moments of the absorption time are extracted from the Laplace-transformed currents as

$$\left\langle T^{\mu}_{\rm exit}(x)\right\rangle_0 = -\partial_s \left[\tilde{J}^{\mu}_{\rm DD}(x,1,s) - \tilde{J}^{\mu}_{\rm DD}(x,0,s)\right]\Big|_{s=0} = \frac{\mathrm{e}^{\mu}(1-x) - \mathrm{e}^{\mu(1-x)} + x}{(\mathrm{e}^{\mu}-1)\,\mu}, \tag{33}$$

$$\int_0^1 \mathrm{d}x\, \left\langle T^{\mu}_{\rm exit}(x)\right\rangle_0 = \frac{\mu\coth\left(\frac{\mu}{2}\right) - 2}{2\mu^2}, \tag{34}$$

$$\left\langle T^{\mu}_{\rm exit}(x)^2\right\rangle_0 = \partial_s^2 \left[\tilde{J}^{\mu}_{\rm DD}(x,1,s) - \tilde{J}^{\mu}_{\rm DD}(x,0,s)\right]\Big|_{s=0},$$

$$\int_0^1 \mathrm{d}x\, \left\langle T^{\mu}_{\rm exit}(x)^2\right\rangle_0 = \frac{\mu^2 + 3\mu^2 \mathrm{csch}^2(\frac{\mu}{2}) - 12}{3\mu^4}. \tag{35}$$

3 Propagator with One Absorbing and One Reflecting Boundary

The propagator with an absorbing (Dirichlet) boundary at $y = 0$ and a reflecting (Neumann) one at $y = 1$ reads

$$P_{\rm DN}(x,y,t) = \sum_{n=-\infty}^{\infty} \frac{(-1)^n}{\sqrt{4\pi t}} \left[\mathrm{e}^{-\frac{(2n+x-y)^2}{4t}} - \mathrm{e}^{-\frac{(2n+x+y)^2}{4t}}\right]. \tag{36}$$

The generalization to include drift is as in Eq. (13). The Laplace transform of Eq. (36) is

$$\tilde{P}_{\mathrm{DN}}(x, y, s) = \sum_{n=-\infty}^{\infty} \frac{(-1)^n \left(\mathrm{e}^{-\sqrt{s}|2n+x-y|} - \mathrm{e}^{-\sqrt{s}|2n+x+y|}\right)}{2\sqrt{s}}$$
$$= \frac{\operatorname{sech}(\sqrt{s})}{2\sqrt{s}}\Big[\sinh\left(\sqrt{s}(x+y-1)\right) - \sinh\left(\sqrt{s}(|x-y|-1)\right)\Big] . \quad (37)$$

It can also be written as

$$\tilde{P}_{\mathrm{DN}}(x, y, s) = \frac{1-\tanh(\sqrt{s})}{\sqrt{s}} \sinh(\sqrt{s}x)\sinh(\sqrt{s}y) + \frac{\mathrm{e}^{-\sqrt{s}|x-y|} - \mathrm{e}^{-\sqrt{s}|x+y|}}{2\sqrt{s}} . \quad (38)$$

Expanding in s, we find

$$\tilde{P}_{\mathrm{DN}}(x, y, s) = \min(x, y) - s\left[xy\frac{(x+y)^3 - |x-y|^3}{12}\right] + \ldots \quad (39)$$

The outgoing current at the lower boundary is

$$\tilde{J}_{\mathrm{DN}}(x, s) = \frac{\cosh\left(\sqrt{s}(1-x)\right)}{\cosh(\sqrt{s})} . \quad (40)$$

Taylor expanding in s yields

$$\tilde{J}_{\mathrm{DN}}(x, s) = 1 - s\left(x - \frac{x^2}{2}\right) + \frac{s^2}{24}(x^4 - 4x^3 + 8x) + \ldots \quad (41)$$

The first term indicates that all trajectories exist, while the time it takes and its second moment are

$$\left\langle T_{\mathrm{exit}}^{\mathrm{DN}}(x)\right\rangle = x - \frac{x^2}{2} , \quad (42)$$
$$\left\langle T_{\mathrm{exit}}^{\mathrm{DN}}(x)^2\right\rangle = \frac{x^4 - 4x^3 + 8x}{12} . \quad (43)$$

The propagator with a Dirichlet boundary condition at the upper, and a Neumann boundary condition at the lower end is obtained by replacing $x \to 1-x$ and $y \to 1-y$.

4 Propagator with Two Reflecting Boundaries

With two reflecting (Neumann) boundary conditions the propagator is

$$P_{\mathrm{NN}}(x, y, t) = \sum_{n=-\infty}^{\infty} \frac{1}{\sqrt{4\pi t}}\left[\mathrm{e}^{-\frac{(2n+x-y)^2}{4t}} + \mathrm{e}^{-\frac{(2n+x+y)^2}{4t}}\right]$$
$$= \frac{1}{2}\vartheta_3\Big(\frac{\pi}{2}(x-y), \mathrm{e}^{-\pi^2 t}\Big) + \frac{1}{2}\vartheta_3\Big(\frac{\pi}{2}(x+y), \mathrm{e}^{-\pi^2 t}\Big) . \quad (44)$$

Laplace transforming yields

$$\tilde{P}_{\mathrm{NN}}(x, y, s) = \frac{\operatorname{csch}(\sqrt{s})}{2\sqrt{s}}\Big[\cosh\big(\sqrt{s}(|x-y|-1)\big) + \cosh\big(\sqrt{s}(x+y-1)\big)\Big] . \quad (45)$$

5 Probabilities for the Span

5.1 The Probability that the Span Reaches 1 for the First Time

The span was defined in Sect. 1, see formulas (4)-(6). We want to know the probability that $S(t)$ becomes 1 for the first time. We note this time by T_1, and its probability distribution by $P_{T_1}(t)$. There are two contributions, depending on whether the process stops while at its minimum or maximum. The probability to stop when the process is at its minimum can be obtained as follows: Consider the outgoing current for the process starting at $X_0 = x$, with the lower boundary positioned at m_1, and the upper boundary at m_2, i.e.

$$\mathbf{J}^{\mu}_{\rm DD}(x, m_1, m_2, t) = \frac{1}{(m_2 - m_1)^2}\, J^{\mu(m_2-m_1)}_{\rm DD}\left(\frac{x - m_1}{m_2 - m_1}, 0, \frac{t}{(m_2 - m_1)^2}\right). \tag{46}$$

(The scale factor can be understood from the observation that the current is a density in the starting point times a spatial derivative of a probability.) The probability that the walk reached m_2 before being absorbed at m_1 is $\partial_{m_2}\mathbf{J}(x, m_1, m_2, t)$. Finally, the probability to have span 1 at time t is this expression, integrated over x between the two boundaries. There is another term, where the process stops while at its maximum. It is obtained from this first contribution when exchanging the two boundaries, and replacing μ by $-\mu$. Setting w.l.o.g. $m_1 = 0$ and $m_2 = m$, the sum of the two terms is

$$\begin{aligned} P^{\mu}_{T_1}(t) &= -\partial_m \frac{1}{m^2}\int_0^m \mathrm{d}x \left[J^{\mu m}_{\rm DD}\left(\frac{x}{m}, 0, \frac{t}{m^2}\right) + J^{-\mu m}_{\rm DD}\left(\frac{x}{m}, 0, \frac{t}{m^2}\right)\right]\Bigg|_{m=1} \\ &= -\partial_m \frac{1}{m}\int_0^1 \mathrm{d}x \left[J^{\mu m}_{\rm DD}\left(x, 0, \frac{t}{m^2}\right) + J^{-\mu m}_{\rm DD}\left(x, 0, \frac{t}{m^2}\right)\right]\Bigg|_{m=1} \\ &= (1 + 2t\partial_t - \mu\partial_\mu)\int_0^1 \mathrm{d}x \left[J^{\mu}_{\rm DD}(x, 0, t) + J^{-\mu}_{\rm DD}(x, 0, t)\right] . \end{aligned} \tag{47}$$

For $\mu = 0$, this simplifies to [13]

$$P_{T_1}(t) = 2(1 + 2t\partial_t)\int_0^1 \mathrm{d}x\, J_{\rm DD}(x, 0, t) \ . \tag{48}$$

Using Eqs. (24) and (13) allows us to rewrite the integral (for $\mu = 0$) as

$$\begin{aligned} \int_0^1 \mathrm{d}x\, J_{\rm DD}(x, 0, t) &= \int_0^1 \mathrm{d}x\, \partial_y \left[\mathbb{P}(x - y, t) - \mathbb{P}(x + y, t)\right]\Big|_{y=0} \\ &= -2\int_0^1 \mathrm{d}x\, \partial_x \mathbb{P}(x, t) = 2\left[\mathbb{P}(1, t) - \mathbb{P}(0, t)\right] . \end{aligned} \tag{49}$$

Thus

$$P_{T_1}(t) = 4(1 + 2t\partial_t)\left[\mathbb{P}(1, t) - \mathbb{P}(0, t)\right] . \tag{50}$$

Inserting the definition (14) of $\mathbb{P}$, we get [13]

$$
\begin{aligned}
P_{T_1}(t) &= 4\big(1 + 2t\partial_t\big) \sum_{n=-\infty}^{\infty} \frac{\mathrm{e}^{-\frac{(2n+1)^2}{4t}} - \mathrm{e}^{-\frac{n^2}{t}}}{\sqrt{4\pi t}} \\
&= \frac{1}{\sqrt{\pi} t^{3/2}} \sum_{n=-\infty}^{\infty} (2n+1)^2 \mathrm{e}^{-\frac{(2n+1)^2}{4t}} - 4n^2 \mathrm{e}^{-\frac{n^2}{t}} \\
&= 4\sqrt{\frac{t}{\pi}}\partial_t \left[\vartheta_2\big(0, \mathrm{e}^{-1/t}\big) - \vartheta_3\big(0, \mathrm{e}^{-1/t}\big)\right] . \qquad (51)
\end{aligned}
$$

With the help of the Poisson-formula transformed Eq. (15) this can be written as [13]

$$
P_{T_1}(t) = 8 \sum_{n=0}^{\infty} \mathrm{e}^{-\pi^2(2n+1)^2 t} \left[2\pi^2(2n+1)^2 t - 1\right] . \qquad (52)
$$

Integrating w.r.t. t, we obtain the probability that the span has not reached 1 at time t,

$$
P^{>}_{T_1}(t) = 8 \sum_{n=0}^{\infty} \mathrm{e}^{-\pi^2(2n+1)^2 t} \left[\frac{1}{\pi^2(2n+1)^2} + 2t\right] . \qquad (53)
$$

This allows us to consider the span of a d-dimensional random walk, defined as the maximum of the span of its d components. The probability that the d-dimensional span has not reached 1 yet is $\left[P^{>}_{T_1}(t)\right]^d$, thus the probability that the d-dimensional span reaches 1 for the first time is

$$
P^d_{T_1}(t) = d P_{T_1}(t) \left[P^{>}_{T_1}(t)\right]^{d-1} . \qquad (54)
$$

The result (52) is compared to a numerical simulation on Fig. 3. Our expansions allow us to give simple formulas for the small and large-t asymptotics,

$$
P_{T_1}(t) \simeq \frac{2\mathrm{e}^{-\frac{1}{4t}}}{\sqrt{\pi} t^{3/2}} + \mathcal{O}(\mathrm{e}^{-\frac{1}{t}}) , \qquad (55)
$$

$$
P_{T_1}(t) \simeq \mathrm{e}^{-\pi^2 t} \left[16\pi^2 t - 8 + \mathcal{O}(\mathrm{e}^{-8\pi^2 t})\right] . \qquad (56)
$$

These expansions work in a rather large, and overlapping domain. Its Laplace transform is [13]

$$
\begin{aligned}
\tilde{P}_{T_1}(s) &= 2(1 + 2s\partial_s) \sum_{n=-\infty}^{\infty} \int_0^{\infty} \mathrm{d}t \, \frac{\mathrm{e}^{-\frac{n^2}{t}} - \mathrm{e}^{\frac{(2n+1)^2}{4t}}}{\sqrt{\pi t}} \mathrm{e}^{-st} \\
&= \frac{1}{\cosh(\sqrt{s}/2)^2} . \qquad (57)
\end{aligned}
$$

Extracting the moments from the Laplace transform yields

$$
\langle T_1 \rangle = \frac{1}{4} , \quad \left\langle T_1^2 \right\rangle = \frac{1}{12} , \quad \left\langle T_1^3 \right\rangle = \frac{17}{480} , \quad \ldots \qquad (58)
$$

Let us now return to the case with drift in Eq. (47). Since formulas become rather cumbersome, we only give one well-converging series expansion, based on the representation (15),

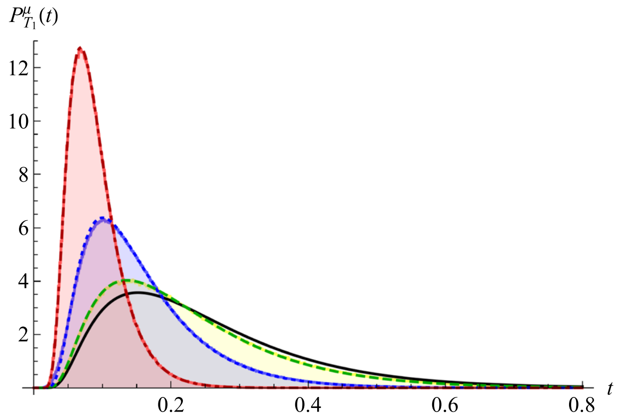

Fig. 3 The function $P^{\mu}_{T_1}(t)$. Lines are as given in Eq. (59). The shaded areas are histograms extracted from numerical simulations of a random walk with time step $\delta t = 10^{-5}$, and 10^6 samples. Black, solid: $\mu = 0$ (numerical test are shown on Fig. 4 of [13]). Green dashed line with yellow histogram: $\mu = 2$. Blue dotted line with blue histogram: $\mu = 5$. Red, dash-dotted and red histogram: $\mu = 10$ (Color figure online)

$$P^{\mu}_{T_1}(t) = \sum_{n=1}^{\infty} a_n^{\mu} + a_n^{-\mu} \tag{59}$$

$$\begin{aligned} a_n^{\mu} = \frac{4\pi^2 n^2 \mathrm{e}^{-\pi^2 n^2 t - \frac{1}{4}\mu(\mu t+2)}}{\left(\mu^2 + 4\pi^2 n^2\right)^2} \Big[& 2\mathrm{e}^{\mu/2}\left(8\pi^4 n^4 t + 2\pi^2 n^2(\mu^2 t - 2) - 3\mu^2\right) \\ & + (-1)^n \left(\mu^2(\mu+6) - 16\pi^4 n^4 t + 4\pi^2 n^2(\mu - \mu^2 t + 2)\right)\Big]. \end{aligned} \tag{60}$$

For $\mu > 0$, the expectation of $\langle T_1 \rangle$ decreases, as does the second moment $\langle T_1^2 \rangle$. Due to the symmetry $\mu \to -\mu$ of Eq. (59), this correction is of order μ^2. Numerical values are

$$\langle T_1 \rangle = \frac{1}{4} - 0.0347\mu^2 + O(\mu^4)\,, \qquad \langle T_1^2 \rangle = \frac{1}{12} - 0.00231\mu^2 + O(\mu^4)\,. \tag{61}$$

Examples for various values of μ are given on Fig. 3.

5.2 Density of the Span

Let us connect to the classical work on the span [5–8]. We will show how to reproduce formulas (3.7)-(3.8) in [7]. The latter give the density $\rho_t(S)$ for the span S at time t. In our formalism, it can be obtained as

$$\rho_t^{\mu}(m_2 - m_1) = -\partial_{m_1}\partial_{m_2} \int_{m_1}^{m_2} \mathrm{d}x \int_{m_1}^{m_2} \mathrm{d}y\, \mathbf{P}^{\mu}_{\mathrm{DD}}(x, y, m_1, m_2, t), \tag{62}$$

where $\mathbf{P}^{\mu}_{\mathrm{DD}}(x, y, m_1, m_2, t)$ is the probability to go from x to y in time t, without being absorbed by the lower boundary positioned at m_1, or the upper boundary positioned at m_2. In terms of the propagator $P^{\mu}_{\mathrm{DD}}(x, y, t)$, this can be written as

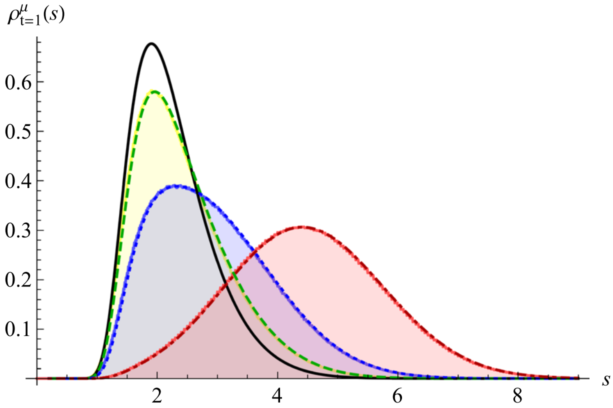

Fig. 4 The density $\rho^{\mu}_{t=1}(s)$, for $\mu = 0$ (black solid line, for a numerical check see Fig. 5 of [13]), $\mu = 1$ (green dashed line, with histogram in yellow), $\mu = 2$ (blue dotted line, histogram in light blue), and $\mu = 4$ (red dot-dashed line, histogram in light red). Numerical validation as for Fig. 3 (Color figure online)

$$\rho^{\mu}_t(S) = \partial_S^2 \left[S \int_0^1 \mathrm{d}x \int_0^1 \mathrm{d}y\, P^{\mu S}_{\mathrm{DD}}(x, y, t/S^2) \right]. \tag{63}$$

We start with $\mu = 0$: Using Eq. (13), and the series expansions (14) and (15) yields after integration and simplifications two different representations,

$$\begin{aligned}\rho_t(S) &= \frac{4}{\sqrt{\pi t}} \sum_{n=1}^{\infty} (-1)^{n+1} n^2 \mathrm{e}^{-\frac{n^2 S^2}{4t}} \\ &= \frac{16t}{S^3} \sum_{n=0}^{\infty} \mathrm{e}^{-\frac{\pi^2 (2n+1)^2 t}{S^2}} \left[\frac{2\pi^2 (2n+1)^2 t}{S^2} - 1 \right].\end{aligned} \tag{64}$$

This is equivalent to Eqs. (3.7–3.8) in [7], if one there replaces $t \to 2t$. (Our variance (2) is $2t$ instead of t as in [7].) The small and large-S asymptotics are

$$\rho_t(S) \simeq \frac{4}{\sqrt{\pi t}} \left[\mathrm{e}^{-\frac{S^2}{4t}} - 4\mathrm{e}^{-\frac{S^2}{t}} + \mathcal{O}\left(\mathrm{e}^{-\frac{9S^2}{4t}}\right) \right], \tag{65}$$

$$\rho_t(S) \simeq \frac{16t}{S^5} \mathrm{e}^{-\frac{\pi^2 t}{S^2}} \left[2\pi^2 t - S^2 \right] + \mathcal{O}\left(s^2 \mathrm{e}^{-\frac{9\pi^2 t}{S^2}} \right). \tag{66}$$

Note that in Eq. (65) we have also retained the subleading term for small S, which considerably improves the numerical accuracy.

Let us now turn to the general case with $\mu \neq 0$. There we have using the generating function (15)

$$\rho^{\mu}_t(S) = \partial_S^2 \sum_{n=1}^{\infty} \frac{32\pi^2 (-1)^{n+1} n^2 S \left[(-1)^n \mathrm{e}^{\frac{\mu S}{2}} - 1 \right]^2 \mathrm{e}^{-\frac{\pi^2 n^2 t}{S^2} - \frac{1}{4}\mu(2S+\mu t)}}{\left(4\pi^2 n^2 + \mu^2 S^2\right)^2}. \tag{67}$$

This formula is checked on Fig. 4. The small-S asymptotics can be obtained by retaining only the leading term in n. Let us finally note that for large μ, this density tends to

$$\rho^{\mu}_t(S) \to \frac{1}{\sqrt{4\pi t}} \left[\mathrm{e}^{-\frac{(S-\mu t)^2}{4t}} + \mathrm{e}^{-\frac{(S+\mu t)^2}{4t}} \right], \qquad |\mu| \gg 0\,. \tag{68}$$

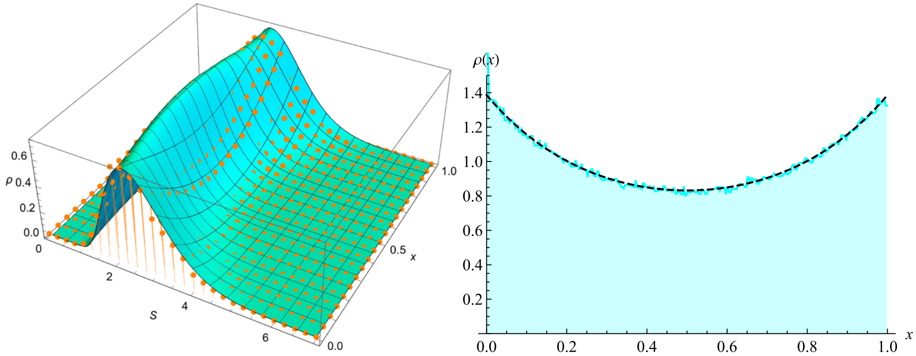

Fig. 5 Left: The density $\rho_{t=1}(S,x)$ as given in Eq. (72). Right: The density $\rho(x)$ as given in Eq. (77). The numerical validation (left: orange dots; right: cyan shaded region) was performed with $\delta t = 10^{-5}$, and 10^6 samples (Color figure online)

For $\mu > 0$, the first term is the probability density for the max of the endpoint, supposing that the minimum is at 0. For $\mu < 0$, the second term arises, with max and min interchanged. Examples and numerical tests are presented on Fig. 4.

6 Joint Density of Maximum and Minimum

We can also derive the joint density of the maximum $M_+ \equiv m_2 > 0$ and minimum $M_- \equiv m_1 < 0$, starting at $x = 0$. In analogy of Eq. (62), this can be written as

$$\rho_t^{\mu}(m_2, m_1) = -\partial_{m_1}\partial_{m_2} \int_{m_1}^{m_2} \mathrm{d}y\, \mathbf{P}_{\mathrm{DD}}^{\mu}(0, y, m_1, m_2, t)\ . \tag{69}$$

The equivalent of Eq. (63) then becomes

$$\rho_t^{\mu}(m_2, m_1) = -\partial_{m_1}\partial_{m_2} \int_0^1 \mathrm{d}y\, P_{\mathrm{DD}}^{\mu(m_2-m_1)}\left(\tfrac{-m_1}{m_2-m_1}, y, \tfrac{t}{(m_2-m_1)^2}\right).$$

Inserting Eq. (13) and one of the two representations (14) or (15) yields two converging series expansions. Since in general these expressions are little enlightening, we continue with $\mu = 0$. To simplify our analysis, we rewrite the density (69) in terms of $S := m_2 - m_1$ and $x := m_1/(m_1 - m_2)$:

$$\rho_t(x, S) := S\rho_t^0\big(-xS, (1-x)S\big)\ . \tag{70}$$

Its marginal density coincides with Eq. (64) ,

$$\int_0^1 \rho_t(x, S)\,\mathrm{d}x = \rho_t(S)\ . \tag{71}$$

The two series expansions in question are

$$\rho_t(S, x) = \frac{4}{S}\sum_{n=0}^{\infty} \mathrm{e}^{-\frac{\pi^2(2n+1)^2 t}{S^2}} \Bigg[\cos\Big((2n+1)x\pi\Big)(2x-1)\left(1 - \frac{2\pi^2(2n+1)^2 t}{S^2}\right)$$

$$+\pi(2n+1)\sin\Big((2n+1)x\pi\Big)\left(\frac{4\pi^2(2n+1)^2t^2}{S^4}+x(1-x)-6\frac{t}{S^2}\right)\Bigg]$$
$$=\frac{1}{\sqrt{\pi t}}\,\partial_x\sum_{n=-\infty}^{\infty}(-1)^n n(n+1)\mathrm{e}^{-\frac{S^2(n+x)^2}{4t}}\,. \tag{72}$$

Interestingly, the latter equation allows us to obtain the marginal distribution of x in closed form. Since this function is independent of t, we drop the time index:

$$\begin{aligned}\rho(x) := \int_0^\infty \mathrm{d}S\,\rho(x,S) &= \partial_x\sum_{n=-\infty}^{\infty}(-1)^n\frac{n(n+1)}{|n+x|}\\ &= 1+\partial_x\left\{\frac{x(1-x)}{2}\left[\psi\left(\frac{2-x}{2}\right)-\psi\left(\frac{3-x}{2}\right)\right.\right.\\ &\qquad\left.\left.-\psi\left(\frac{x+1}{2}\right)+\psi\left(\frac{x+2}{2}\right)\right]\right\}.\end{aligned} \tag{73}$$

This is the density for the relative location of the starting point w.r.t. the domain given by the maximum and minimum. It is also the distribution of the final position w.r.t. the same domain. This density is larger at the boundaries, as is easily understood: After a new record, the particle diffuses away from the record, but the probability density remains higher close to the last record.

We finally note that a similar question has been asked in reference [20] (see also [3]).

7 The Span with One Reflecting Boundary

Now consider diffusion with a reflecting wall at $x = 0$. We want to know the probability density for the span to reach 1 for the first time. For simplicity, we restrict to the drift-free case $\mu = 0$. We also assume $x < 1$, since for $x > 1$ the reflecting boundary can never be reached, and we recover the result of Sect. 5.1. Suppose the process starts at x, with $0 \le x < 1$. There are two possibilities: Either the process first reaches 0, or 1. The probabilities for these two events are x and $1 - x$, respectively. If it first reaches 1, then it almost surely also reaches $1 + \delta$ with δ small before its span becomes 1; as a consequence its minimum is bounded by δ. Thus it never reaches the lower boundary at $x = 0$.

Consider the two contributions in turn: The first contribution, when the process never reaches $x = 0$, is similar to the one obtained in Eq. (47). It can itself be decomposed into two sub-contributions, depending on whether, when the span reaches 1, X_t equals its maximum (case 1a) or minimum (case 1b). We start with case 1a. Denoting $\mathbf{J}_{\rm DD}(y, m_2, t|m_1, m_2)$ the outgoing current at the upper boundary m_2, for a particle starting at y, with lower boundary m_1, we have

$$\begin{aligned}p_{1a}(x,t) &= -\int_0^x \mathrm{d}y\,\partial_{m_1}\mathbf{J}_{\rm DD}(y,m_2,t|m_1,m_2)\Big|_{m_2=m_1+1}\\ &= -\int_0^x \mathrm{d}y\,\partial_{m_1}\left[\frac{1}{(m_2-m_1)^2}J_{\rm DD}\left(\frac{y-m_1}{m_2-m_1},1,\frac{t}{(m_2-m_1)^2}\right)\right]_{m_1=0}^{m_2=1}.\end{aligned} \tag{74}$$

Let us first evaluate its normalization, using that the time-integrated current is the exit probability,

$$\int_0^\infty \mathrm{d}t\, p_{1a}(x,t) = -\int_0^x \mathrm{d}y\, \partial_{m_1} \frac{y-m_1}{m_2-m_1}\bigg|_{m_1=0}^{m_2=1} = \int_0^x \mathrm{d}y\,(1-y) = x - \frac{x^2}{2}\ . \tag{75}$$

Note that this is smaller than the probability x to exit at the upper boundary. This can be understood from the fact that the trajectory has to go beyond 1, or more precisely to $1+\min$, where $\min > 0$ is the minimum of the trajectory. Continuing with Eq. (74), we obtain

$$p_{1a}(x,t) = 2\int_0^x \mathrm{d}y \Big[-2\partial_y \mathbb{P}(1-y,t) - 2\partial_y\partial_t \mathbb{P}(1-y,t) + (1-y)\partial_y^2 \mathbb{P}(1-y,t)\Big]. \tag{76}$$

Integrating this yields

$$\begin{aligned} p_{1a}(x,t) =& 2\Big[\mathbb{P}(1,t) - \mathbb{P}(1-x,t)\Big] + 4t\partial_t\Big[\mathbb{P}(1,t) - \mathbb{P}(1-x,t)\Big] \\ &+ 2\partial_y \mathbb{P}(y,t)|_{y=1} + 2(1-x)\partial_x \mathbb{P}(1-x,t)\ . \end{aligned} \tag{77}$$

(The first term on the last line vanishes). To simplify this expression, introduce the function $\mathbb{R}(x,t)$ defined as

$$\mathbb{R}(x,t) := -2\Big[1 + 2t\partial_t - (1-x)\partial_x\Big]\mathbb{P}(1-x,t)\ . \tag{78}$$

For later reference we also give its Laplace transform

$$\begin{aligned} \tilde{\mathbb{R}}(x,s) &= 2\Big[1 + 2s\partial_s + (1-x)\partial_x\Big]\tilde{\mathbb{P}}(1-x,s) \\ &= -\frac{\cosh\big(\sqrt{s}(1-x)\big)}{\sinh(\sqrt{s})^2}\ . \end{aligned} \tag{79}$$

Eq. (77) becomes

$$p_{1a}(x,t) = \mathbb{R}(x,t) - \mathbb{R}(0,t)\ . \tag{80}$$

This is written s.t. $\mathbb{R}$ can be thought of as the principal function of the integrand in Eq. (76). The second contribution where the process never reaches 0 is obtained when the process has its maximum at $1+\delta$ with $\delta > 0$, before going down to $\delta < x$, where the process stops (case 1b). By symmetry, this is the same expression as Eq. (74), where all positions x are sent to $1-x$, i.e.

$$\begin{aligned} p_{1b}(x,t) &= -\int_{1-x}^{1} \mathrm{d}y\, \partial_{m_1} \mathbf{J}_{\mathrm{DD}}(y, m_2, t|m_1, m_2)\Big|_{m_2=m_1+1} \\ &= -\int_{1-x}^{1} \mathrm{d}y\, \partial_{m_1}\left[\frac{1}{(m_2-m_1)^2} J_{\mathrm{DD}}\left(\frac{y-m_1}{m_2-m_1}, 1, \frac{t}{(m_2-m_1)^2}\right)\right]_{m_1=0}^{m_2=1}. \end{aligned} \tag{81}$$

The probability for this process is as in Eq. (75) given by the time-integrated current

$$\int_0^\infty \mathrm{d}t\, p_{1b}(x,t) = -\int_{1-x}^1 \mathrm{d}y\, \partial_{m_1} \frac{y-m_1}{m_2-m_1}\bigg|_{m_1=0}^{m_2=1} = \int_{1-x}^1 \mathrm{d}y\,(1-y) = \frac{x^2}{2}\ . \tag{82}$$

Thus, as expected

$$\int_0^\infty \mathrm{d}t\, p_1(x,t) = \int_0^\infty \mathrm{d}t\, p_{1a}(x,t) + p_{1b}(x,t) = x\ . \tag{83}$$

Let us continue with the evaluation of $p_{1b}(x,t)$,

$$p_{1b}(x,t) = 2\int_{1-x}^1 \mathrm{d}y \Big[-2\partial_y \mathbb{P}(1-y,t) - 2\partial_y \partial_t P(1-y,t) + (1-y)\partial_y^2 P(1-y,t)\Big]. \tag{84}$$

Integration yields

$$p_{1b}(x,t) = 2\Big[\mathbb{P}(x,t) - \mathbb{P}(0,t)\Big] + 4t\partial_t\Big[\mathbb{P}(x,t) - \mathbb{P}(0,t)\Big] + 2x\partial_x \mathbb{P}(x,t)\ . \tag{85}$$

In analogy of Eq. (80) this can be written as

$$p_{1b}(x,t) = \mathbb{R}(1,t) - \mathbb{R}(1-x,t)\ . \tag{86}$$

The sum of the two contributions p_{1a} and p_{1b} is

$$\begin{aligned} p_1(x,t) &= p_{1a}(x,t) + p_{1b}(x,t) \\ &= 2(1+2t\partial_t)\,[\mathbb{P}(1,t) - \mathbb{P}(0,t) + \mathbb{P}(x,t) - \mathbb{P}(1-x,t)] \\ &\quad +2x\partial_x \mathbb{P}(x,t) + 2(1-x)\partial_x \mathbb{P}(1-x,t) \\ &= \mathbb{R}(x,t) - \mathbb{R}(0,t) - \mathbb{R}(1-x,t) + \mathbb{R}(1,t)\ . \end{aligned} \tag{87}$$

Note that for $x = \frac{1}{2}$, one gets $p_1(x,t) = \frac{1}{2} P_{T_1}(t)$.

The second contribution is achieved when the process first reaches the lower boundary. It can be obtained by folding the probability to first reach the lower boundary, i.e. the outgoing current at $x = 0$, with an absorbing boundary both at $x = 0$ and $x = 1$, with the outgoing current at $x = 1$ with a reflecting boundary at $x = 0$ and an absorbing one at 1, i.e.

$$p_2(x,t) = -\int_0^t \mathrm{d}\tau\, J_{\mathrm{DD}}(x,0,\tau) J_{\mathrm{ND}}(0,1,t-\tau)\ . \tag{88}$$

Passing to Laplace variables, this reads

$$\tilde{p}_2(x,s) = -\tilde{J}_{\mathrm{DD}}(x,0,s)\tilde{J}_{\mathrm{ND}}(0,1,s)\ . \tag{89}$$

We had calculated the currents before,

$$-\tilde{J}_{\mathrm{DD}}(x,0,s) = \frac{\sinh\big(\sqrt{s}(1-x)\big)}{\sinh(\sqrt{s})}\ , \tag{90}$$

$$\tilde{J}_{\mathrm{ND}}(0,1,s) = \frac{1}{\cosh(\sqrt{s})}\ . \tag{91}$$

This allows us to simplify $\tilde{p}_2(x,s)$ as

$$\tilde{p}_2(x,s) = \frac{2\sinh\big(\sqrt{s}(1-x)\big)}{\sinh(2\sqrt{s})}\ . \tag{92}$$

The inverse Laplace transform of Eq. (89) can be written as

$$p_2(x,t) = \sum_{n=-\infty}^{\infty} \frac{\mathrm{e}^{-\frac{(1-4n+x)^2}{4t}}(1-4n+x)}{\sqrt{\pi}t^{3/2}}$$

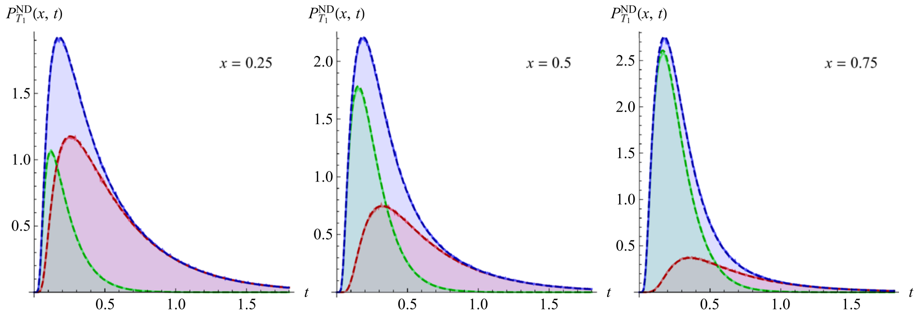

Fig. 6 The probability $P_{T_1}(t)$ with a reflecting boundary at 0, and an absorbing one at 1, for $x = 0.25$, $x = 0.5$, and $x = 0.75$. The green contribution is $p_1(x,t)$, while the red one is $p_2(x,t)$. Their sum is given in blue. The dark dashed lines are the analytic curves, while the numerical data are given as shaded regions with their envelope in the same color. 10^7 samples where simulated, with a time-step of $\delta t = 10^{-5}$ (Color figure online)

$$= -\partial_x \vartheta_3\left(-\frac{\pi}{4}(x+1), \mathrm{e}^{-\frac{\pi^2 t}{4}}\right) = -2\,\partial_x\, \mathbb{P}\left(\frac{1+x}{2}, \frac{t}{4}\right). \tag{93}$$

This is checked by evaluating the Laplace transform of each term in the above sum, and then performing the sum over n.

The probability to first reach the lower boundary is

$$\int_0^\infty \mathrm{d}t\; p_2(x,t) = 1 - x\ . \tag{94}$$

The probability to reach span 1, starting at x, and with a reflecting boundary at $x = 0$ is finally obtained as

$$P^{\mathrm{ND}}_{T_1}(x,t) = p_1(x,t) + p_2(x,t)\ . \tag{95}$$

The mean time to reach span 1 is

$$\left\langle T^{\mathrm{ND}}_1(x)\right\rangle = \frac{1}{2} - \frac{x^2}{4}\ . \tag{96}$$

Thus when starting close to the reflecting wall, it takes on average twice as long to reach span 1, as when starting from far away.

A numerical check for $x = 0.25$, $x = 0.5$, and $x = 0.75$ is presented on Fig. 6.

8 The Span with Two Reflecting Boundaries

Finally, consider two reflecting (Neumann) boundaries at $x = 0$ and $x = a \geq 1$, and suppose that $0 < x < 1$, and $0 < a - x < 1$, so that both boundaries can be reached before the span attains one and the process terminates. These conditions can be summarized in

$$a - 1 < x < 1\ . \tag{97}$$

In generalization of Eq. (93), one can write

$$P^{\mathrm{NN}}_{T_1}(x,t) = p_2(x,t) + p_2(a-x,t) + p_3(x,t|a) + p_3(a-x,t|a)\ . \tag{98}$$

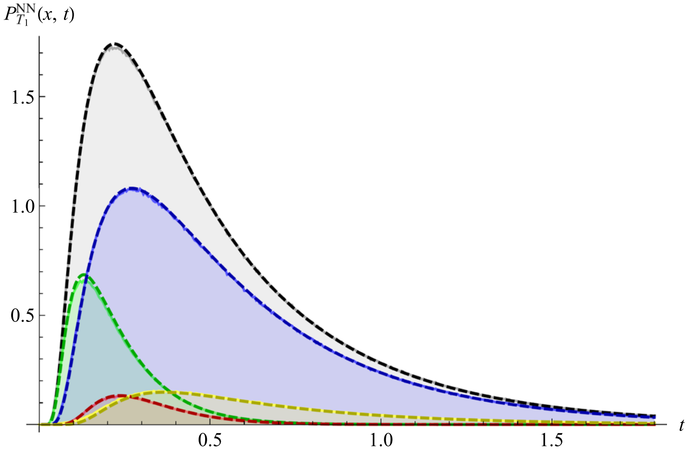

Fig. 7 The probability $P_{T_1}^{\mathrm{NN}}(x,t)$, for $x = 0.3$, $a = 1.2$ (black). The contributions are $p_2(x,t)$ (blue), $p_2(a-x,t)$ (yellow), $p_3(x,t|a)$ (green), and $p_3(a-x,t|a)$ (red). Numerical simulations (Color figure online)

The function $p_3(x,t|a)$ is a modification of $p_{1a}(x,t)$, defined by

$$\begin{aligned} p_3(x,t|a) &= 2\int_{\max(0,1+x-a)}^{x} \mathrm{d}y \Big[-2\partial_y \mathbb{P}(1-y,t) - 2\partial_y\partial_t \mathbb{P}(1-y,t) + (1-y)\partial_y^2 \mathbb{P}(1-y,t) \Big] \\ &= \mathbb{R}(x,t) - \mathbb{R}\big(\max(0,1+x-a),t\big)\,. \end{aligned} \tag{99}$$

This integral is analogous to (76), with the difference that the lower boundary may be larger than 0; this domain of integration is restricted s.t. the process never touches the lower boundary. For $a \geq 1+x$, this reproduces the probability $p_{1a}(x,t)$,

$$p_{1a}(x,t) = p_3(x,t|a)\Big|_{a\geq 1+x}\,. \tag{100}$$

Using our assumptions, $p_3(x,t|a)$ can be simplified to

$$p_3(x,t|a) = \mathbb{R}(x,t) - \mathbb{R}(1+x-a,t\big)\,. \tag{101}$$

To get to the last line we used our assumption (97).

Similarly, the last term in Eq. (98) reproduces the function $p_{1b}(x,t)$ used above, when choosing

$$p_{1b}(x,t) = p_3(a-x,t|a)\Big|_{a=1+x}\,. \tag{102}$$

Note that Eq. (98) has manifestly the symmetry $x \to a-x$, both for p_2 and p_3. Choosing $a = 1+x$, the sum of the latter terms becomes $p_{1a}(x,t) + p_{1b}(x,t)$, making manifest the hidden symmetry between these terms.

One also checks that for x satisfying condition (97), $\int_0^\infty \mathrm{d}t\, P_{T_1}^{\mathrm{NN}}(x,t) = 1$, thus the probability (98) is properly normalized. A numerical test is presented on Fig. 7.

Finally, the Laplace transform of $P_{T_1}^{\mathrm{NN}}(x,t)$ can be evaluated using Eqs. (79) and (92) above. After simplification, and assuming condition (97), we obtain

$$\tilde{P}_{T_1}^{\mathrm{NN}}(x,s) = \frac{\cosh\!\left(\frac{a\sqrt{s}}{2}\right)\cosh\!\left(\frac{(a-2x)\sqrt{s}}{2}\right)}{\cosh^2\!\left(\frac{\sqrt{s}}{2}\right)\cosh(\sqrt{s})}\,. \tag{103}$$

Taylor expanding, we find for the first two connected moments

$$\left\langle T_1^{\mathrm{NN}}(x)\right\rangle = \frac{1}{4}\left(3-\frac{a^2}{2}\right)-\frac{1}{2}\left(x-\frac{a}{2}\right)^2 , \tag{104}$$

$$\left\langle \left[T_1^{\mathrm{NN}}(x)\right]^2\right\rangle^{\mathrm{c}} = \frac{3}{16}-\frac{a^4}{96}-\frac{1}{6}\left(x-\frac{a}{2}\right)^4 . \tag{105}$$

9 Open Problems

For motivations for the questions asked here, and applications of the results, we refer the reader to the introduction. What are the open problems? Let us come back to the image of a myopic foraging rabbit, and ask when it is no longer hungry. Suppose there is a uniform food distribution. The rabbit starts with an empty stomach, does a Brownian motion and eats everything it can get, until its stomach is full ($S = 1$). The probability for this time is the probability that the span reaches one for the first time, as given in Eq. (50), and after. But a real rabbit is burning food, so add a (negative) drift, i.e. stop when $S(t) - \mu t = 1$. Curiously, this problem is much more difficult to solve, and we (currently) have no analytical solution. One may be able to calculate the probability that the rabbit dies before having a full stomach, following the approach outlined in Ref. [12].

Another open problem is the generalization of the observables obtained here for correlated processes, as fractional Brownian motion. While the first moments of the span distribution have been obtained in an expansion [13] around $H = 1/2$ (Brownian motion), the full distribution remains to be evaluated.

Note added in Proof After completion of this work we learned that for the drift-free case the time that the span first reaches one was already calculated in Phys. Rev. E 94, 062131 (2016).

References

1. Feller, W.: Introduction to Probability Theory and Its Applications. Wiley, New York (1950)
2. Redner, S.: A Guide to First-Passage Problems. Cambridge University Press, Cambridge (2001)
3. Borodin, A.N., Salminen, P.: Handbook of Brownian Motion—Facts and Formulae. Birkhäuser, Boston (2002)
4. Weiss, G.H., DiMarzio, E.A., Gaylord, R.J.: First passage time densities for random walk spans. J. Stat. Phys. **42**, 567–572 (1986)
5. Palleschi, V., Torquati, M.R.: Mean first-passage time for random-walk span: comparison between theory and numerical experiment. Phys. Rev. A **40**, 4685–4689 (1989)
6. Daniels, H.E.: The probability distribution of the extent of a random chain. Math. Proc. Camb. Philos. Soc. **37**, 244–251 (1941)
7. Feller, W.: The asymptotic distribution of the range of sums of independent random variables. Ann. Math. Stat. **22**, 427–432 (1951)
8. Weiss, G.H., Rubin, R.J.: The theory of ordered spans of unrestricted random walks. J. Stat. Phys. **14**, 333–350 (1976)
9. Annesi, B., Marinari, E., Oshanin, G.: Covariance of the running range of a Brownian trajectory, (2019), arXiv:1902.06963
10. Rager, C.L., Bhat, U., Bénichou, O., Redner, S.: The advantage of foraging myopically. J. Stat. Mech. **2018**, 073501 (2018)
11. Cannon, J.R.: The One-Dimensional Heat Equation. Encyclopedia of Mathematics and Its Applications, vol. 23. Department of Mathematics, MIT, Cambridge (1984)

12. Bray, A.J., Smith, R.: Survival probability of a diffusing particle constrained by two moving, absorbing boundaries. J. Phys. A **40**, F235 (2007). cond-mat/0612563
13. Wiese, K.J.: First passage in an interval for fractional Brownian motion. Phys. Rev. E **99** 032106, (2018) arXiv:1807.08807
14. Wergen, G., Bogner, M., Krug, J.: Record statistics for biased random walks, with an application to financial data, Phys. Rev. E **83** 051109, (2011) arXiv:1103.0893
15. Mirny, L., Slutsky, M., Wunderlich, Z., Tafvizi, A., Leith, J., Kosmrlj, A.: How a protein searches for its site on DNA: the mechanism of facilitated diffusion. J. Phys. A **42**, 434013 (2009)
16. Nourdin, I.: Selected Aspects of Fractional Brownian Motion. Bocconi & Springer Series, New York (2012)
17. Dieker, A.B.: Simulation of fractional Brownian motion, www.columbia.edu/~ad3217/fbm/thesis.pdf PhD thesis, University of Twente, (2004)
18. Krug, J.: Persistence of non-Markovian processes related to fractional Brownian motion. Markov Process. Relat. Fields **4**, 509–516 (1998)
19. Sadhu, T., Delorme, M., Wiese, K.J.: Generalized arcsine laws for fractional Brownian motion. Phys. Rev. Lett. **120**, 040603 (2018). https://doi.org/10.1103/PhysRevLett.120.040603
20. Salminen, P., Vallois, P.: On maximum increase and decrease of Brownian motion. Ann. Inst. Henri Poincaré PR **43**, 655–676 (2007)